NOTE 9C

Version 2
artwork inclusion 25.01.2014
Version 1‡
posted 03.01.2014

ANGULAR MOMENTA OF THE SOLAR SYSTEM

C. INVOLVEMENT OF THE SUN

Luc Fraiture†

1. INTRODUCTION

The purpose of this note is to perform an initial investigation in order to find potential consequences hidden in solar sun spot activity which could be due to the the variable body **A**ngular **M**oment**a** (AMa) in the solar system which have been presented in note 9A. In this respect we will consider the sun separately as point mass as well as three dimensional body without making any assumptions on its interior behaviour. This means that no attempt will be made to make a link with established solar activity features concerning the structure and the present knowledge about the dynamics of the solar interior, see for instance R. Howe(2009) and P. Charbonneau(2010).

The conventional rotational dynamics theory of the sun has historically got little attention. One and a half century ago R.C. Carrington, see J.G. Beck and P. Giles(2005) and references therein, was, in our opinion, the first to study a pure dynamical property of the sun, namely its spin rate and its inertial orientation or spin axis. The idea that tidal effects could play a role at the level of the photosphere in the mechanism giving rise to sun spots was already abandoned in the beginning of the twentieth century, because the orbital period of Jupiter and the mean sun spot cycle period were not compatible. On top of this, the tidal acceleration is approximately 10^{12} times smaller than the pure gravitational acceleration on the solar surface, see C.N. Anderson (1956). This was not the last word! In a remarkable paper by Abreu et al.(2012) it is shown that planetary tidal forces and resulting torques acting on the tachocline inside the sun lead to repeating longer intervals with specific activity patterns with periods between 88 and 550 years (without excluding the existence of longer periods). This was achieved by studying the traces of cosmogenic radionuclides found in probes covering at least 10,000 years of recent Earth history.

---

‡ This note is derived from a paper proposal to the 'Journal of Atmospheric and Solar-Terrestrial Physics' in the first half of 2013. The first part of this attempt contained a description of the conjecture about the link between body and mass point angular momenta, but without the plausibility background now given in note 9A. The conjecture was an essential reason of rejection by one referee who did understandably not take the risk for something which had not almost reached the level of certainty. The part dealing with the sun presented here, has been taken from that submission with minor complements and a rephrasing of the conclusions.

† Private contribution; address: Lucasweg 6, D-64287 Darmstadt, Germany

Although solar physics was very successful all along the twentieth century, as one can read in the recent book of K.R. Lang(2000), conventional dynamics did not participate in this expansion of solar science. We only note a paper by Jose(1965), who presented the rotational dynamics of the sun in the way it was still historically understood. He studied the evolution of the size of the sun's inertial position and velocity vector as well as a tentative value of the variable **A**ngular **M**omentu**m** (AMm) *magnitude* and its derivative, involving the radius of curvature of the solar inertial motion. Exactly this last fact seems inadequate, because it implies an approximation of more or less unknown nature. Although the total AMm magnitude was derived correctly, splitting off the variable AMm and **T**o**RQ**ues (TRQ)s lacked a solid dynamical background and could therefore not reasonably clarify the link to the planetary influences. Notwithstanding, no valid alternatives were presented in the meanwhile.

In the first decade of the present century a number solar physicists indirectly or directly expressed their concern about the level of knowledge of the solar gyro-dynamics. We especially think at D. Jucket(2003) who spelled out in detail the presently open points about the topic. Also I.R.G. Wilson et al.(2008) voiced the lack of comfortable background in the area of solar conventional rotational dynamics. Finally, C. de Jager and G.J.M. Versteegh(2005) gave orders of magnitude required for TRQs to be able to play some role in solar activity, and at the same occasion they deplored the unavailability of any known theoretical evidence supporting their existence. The main purpose of the present paper is to analyze whether the tentative dynamical theory given in note 9A allows us to give this simple dynamical background.

The main novelty which is introduced in note 9A concerns the ability to analytically break down the inertial AMa of the sun and the solar system planets into their variable and constant parts. This relies on the fact that one can perform a very basic transformation of the inertial AMa, so as to explicitly contain the heliocentric vector products of the *individual* planetary heliocentric positions and time derivatives of the mass points representing these bodies. But, these vector products are constant by Kepler's second law. The sum of these particular vectors corresponds to the constant part of the AMm which can thus be split off. The further problem which was unsolved so far was the link between a variable mass point and the extended body AMm reaction. We derived that the AMm of the solar system can hardly be constant if TRQs corresponding to the mass point and body momenta are not both at each instant equal in magnitude and opposite in sign, even if the bodies involved are not (completely) rigid. This is very plausible, but remains a conjecture as long as we cannot identify a process in the solar system which is only explainable by employing this hypothesis.

Our note is organized as follows. In the next sections we shortly refer to the results presented in note 9A, but now addressed to the sun in particular. The inherent theoretical properties of the solar AMm and TRQ are analyzed in section 4. In contrast, section 5 is devoted to rudimentary comparisons of sun spot activity with TRQs and energy, making use of both the conventionally smoothed as well as monthly mean sun spot records, downloaded from publicly available files of the Solar Influence Data Center in Brussels.

2 THE VARIABLE ANGULAR MOMENTUM OF THE SUN

Although we will employ the same notations as those used in note 9A, we summarise here the essentials related to the sun in order to be self contained.

Let M_{sun} be the mass and $\mathbf{r_{sun}}$ the position vector of the sun with respect to the barycenter and let M_i with $\mathbf{r_i}$ similarly be the masses and barycentric positions of the planets with the indices $i = 1$ to 8 counting up from Mercury with $i = 1$ to Neptune with $i = 8$, respectively. The instantaneous position vector of the planet i with respect to the sun center will be identified by $\mathbf{r_{i,h}}$, where the subscript h stands for 'heliocentric'.

The units in tables and plots presented in this note will rely the astronomical unit AU $= 149.598\,10^6$ km as length unit. Except if specified otherwise, the masses are measured in Earth masses (EM). For example: $M_{sun} = 332270.$ EM. An important number in this respect is the total mass M_{tot} of the solar system which is approximated by 332716.7 EM. The normalized dimensionles planetary masses are represented by $m_i = M_i/M_{tot}$ for any planet i. For the unit of time we use the terrestrial solar 'day', if not explicitly replaced by 'yr'. We will call them 'plotting units'.

The moment arm of the inertial AMm of the sun as point mass is $\mathbf{r_{sun}}$ and its AMm is to be represented by

$$\mathbf{D_s} \;=\; M_{sun}\,(\mathbf{r_{sun}} \times \dot{\mathbf{r}}_{\mathbf{sun}}) \tag{1}$$

by definition. Its time derivative, identified by a dot, is the corresponding TRQ. It is equal to

$$\dot{\mathbf{D}}_{\mathbf{s}} \;=\; M_{sun}\,(\mathbf{r_{sun}} \times \ddot{\mathbf{r}}_{\mathbf{sun}}) \tag{2}$$

Let us now introduce the abbreviation

$$\mathbf{p_{jk}} \;=\; m_j\, m_k\,(\mathbf{r_{j,h}} \times \dot{\mathbf{r}}_{\mathbf{k,h}} \,+\, \mathbf{r_{k,h}} \times \dot{\mathbf{r}}_{\mathbf{j,h}}) \tag{3}$$

for what we will call the mixed momentum of the bodies j and k, with $\mathbf{p_{jk}} = \mathbf{p_{kj}}$ and $\mathbf{p_{kk}} = m_k^2\,\mathbf{r_{k,h}} \times \dot{\mathbf{r}}_{\mathbf{k,h}}$. Adequate manipulation of (1) yields the constant part:

$$\mathbf{D_{sc}} \;= M_{sun} \sum_{i=1}^{8} \mathbf{p_{ii}} \tag{4}$$

and for the variable part we obtain:

$$\mathbf{D_{sv}} \;= M_{sun} \sum_{i=1}^{8} \sum_{j=i+1}^{8} \mathbf{p_{ij}} \tag{5}$$

By analyzing the time dependency of (3) for $k \neq j$ it appears that the period corresponding to the fundamental frequency of $\mathbf{p_{ij}}$, is equal to the synodic period T_{ij} of the planets i and j. We may further assume that the contribution of the inner planets to (5) can be neglected. Therefore, in all what follows, the numerical evaluation of (5) and its derivative is based on the planets 5 to 8 only.

For the sake of completeness we add hereafter the synodic periods of the Jovian planet pairs.

Table 1. Periods (yr) of the synodic frequencies of the Jovian Planets

REF	PERIOD	REF	PERIOD	REF	PERIOD
T_{58}	12.782	T_{57}	13.812	T_{56}	19.859
T_{68}	35.871	T_{67}	45.364	T_{78}	171.41

If we speculate that the common action of the four Jovian planets is a function of geometry, we may assume that these common patterns have periods which are represented by the higher order synodic period of two planet pairs. We actually mean the periods

$$\begin{aligned} \frac{1}{T_{57/68}} &= \frac{1}{T_{57}} - \frac{1}{T_{68}} = (\frac{1}{T_5} - \frac{1}{T_7}) - (\frac{1}{T_6} - \frac{1}{T_8}) \\ &= (\frac{1}{T_5} - \frac{1}{T_6}) - (\frac{1}{T_7} - \frac{1}{T_8}) = \frac{1}{T_{56/78}} = \frac{1}{22.46} \end{aligned} \tag{6}$$

and $T_{58/67} = 17.80$. In words, $T_{56/78}$ says that the period separating simultaneous conjunction of the pair Jupiter/Saturn and the conjunction of Uranus/Neptune is 22.46 yr. This period also applies to $T_{57/68}$, namely the period separating simultaneous conjunction of the pair Jupiter/Uranus and the conjunction of Saturn/Neptune It happens that 22.5 yr is the approximate mean Hale cycle period for the complete magnetic activity cycles of the sun, see P.R. Wilson(1994). This simple but nevertheless remarkable result points to a link between the solar magnetohydrodynamics and conventional dynamics relying on consequences of the proposed mass point - body coupling. The fact that the first harmonic period of T_{67}, namely $0.5\,T_{67}$, is equal to 22.68 yr also supports this indication.

In note 9A we draw the attention to the fact that these (Jovian) synodic periods have an approximate common multiple equal to 178.5 years. Moreover, this is also the separation time of the well known periodical occurrence of a three-foil trajectory segment of the sun, see Charvatova and Střeštík (1991). This three-foil is normally centered closely to the solar system's barycenter. Running through this configuration takes some 50 years. This is an aspect we have given special consideration in this note.

3. ABOUT ROTATIONAL ENERGY

In the present context the rotational energy contains two separate elements, namely the mass point energy and the three dimensional body energy. In the case of the sun the rotational kinetic energy of the mass point can only partly be compensated by a potential energy, because part of the AMm is not constant and the barycenter is not the location of a central force acting upon the sun. Moreover, the oscillating variable AMm fraction affects this mass point kinetic energy in an important manner. It is creating unusual velocity accelerations which are not comparable with what happens with the planets. The question can be asked whether these accelerations are not causing pseudo-tidal forces inside the non-rigid sun. Also this is a question we will not deal with here, but we will see in section 5, that the mass point energy plots show some peculiarities which suggest a potential contribution to solar activity energy.

Let us start with the total instantaneous solar mass point rotational energy hidden in the trajectory of the sun. Therefore, we need the angular velocity $\mathbf{\Omega_s}$ of the sun which is equal to:

$$\mathbf{\Omega_s} \;=\; \frac{\mathbf{r_{sun}} \times \dot{\mathbf{r}}_{\mathbf{sun}}}{||\mathbf{r_{sun}}||^{\mathbf{2}}} \tag{7}$$

by definition. Consequently, the total kinetic rotational mass point energy $\mathrm{E_{tot}}$ is simply equal to

$$\begin{aligned} \mathrm{E_{tot}} \;&=\frac{1}{2}\,\mathbf{\Omega_s}\cdot\mathbf{D_s} \;=\; \frac{||\mathbf{D_s}||^{\mathbf{2}}}{2\,M_{sun}||\mathbf{r_{sun}}||^{\mathbf{2}}} \\ &= \frac{||\mathbf{D_{sc}}||^{\mathbf{2}} \,+\, \mathbf{2}\,\mathbf{D_{sc}}\cdot\mathbf{D_{sv}} \,+\, ||\mathbf{D_{sv}}||^{\mathbf{2}}}{2\,M_{sun}||\mathbf{r_{sun}}||^{\mathbf{2}}} \end{aligned} \tag{8}$$

where $\mathbf{a}\cdot\mathbf{b}$ denotes the inner or scalar product between the vectors $\mathbf{a}$ and $\mathbf{b}$. The presence of r_{sun} in the denominator of (8) means that also $||\mathbf{D_{sc}}||^{\mathbf{2}}$ in the numerator contributes to the kinetic energy variations, but we assume that it takes place in a way similar to energy variation for a Keplerian orbit. The mass point kinetic energy where the sun's variable AMm fraction is directly involved, is given by:

$$\mathrm{E_{var}} \approx \frac{\mathbf{2}\,\mathbf{D_{sc}}\cdot\mathbf{D_{sv}} \,+\, ||\mathbf{D_{sv}}||^{\mathbf{2}}}{2\,M_{sun}||\mathbf{r_{sun}}||^{\mathbf{2}}} \tag{9}$$

Plots (Figs. 3,4,5,7,8) of mass point energy do not contain separate curves for $\mathrm{E_{var}}$ just defined. While (8) must always remain positive or zero, $\mathrm{E_{var}}$ in (9) may become negative, because it is always satisfying $0 \le \mathrm{E_{tot}} - \mathrm{E_{var}}$.

If we now turn to the sun as three dimensional body it is clear that $\mathbf{\Omega_s}$ cannot be employed to isolate the kinetic body energy prescribed by the body compensation AMm axiom of note 9A. This axiom only says that in this case the extended solar body is subject to a TRQ equal to $\dot{\mathbf{B}}_\mathbf{s} = -\dot{\mathbf{D}}_\mathbf{sv}$. No other link to the trajectory is assumed.

With $\mathbf{B_s}$ at hand we can only proceed if we have the instantaneous inertia tensor $\mathbf{N_s}$ of the sun at our disposition, for then we can compute an equivalent angular velocity $\mathbf{\Omega_v} = \mathbf{N_s^{-1}B_s}$. Consequently, the equivalent body energy is equal to:

$$\mathrm{E}_{body} \;=\; \mathbf{B_s'}\,\mathbf{N_s^{-1}}\,\mathbf{B_s} \tag{10}$$

where the accent means transposition as conventionally employed in matrix algebra.

On this basis we can derive a crude approximate 'body' energy $\mathrm{E_{bod}}$ by assuming that the sun would be a rigid homogeneous and fully symmetric sphere of radius ρ_s. If the sun was such a body, its spin inertia I_{sun} would be equal to $0.4\,M_{sun}\,\rho_s^2$ around any axis through the sun center. If ω_v is the angular velocity of this sun around its instantaneous spin axis, its 'variable' AMm can be approximated by:

$$|D_{sv}| \approx \frac{2}{5}\,M_{sun}\,\rho_s^2\,\omega_v \tag{11}$$

which allows us to compute ω_v. Hence, the approximate instantaneous rotational body energy $\mathrm{E_{bod}}$ is equal to

$$\mathrm{E_{bod}} \;=\; \frac{1}{2}\,I_{sun}\,\omega_v^2 \;=\; \frac{5\,D_{sv}^2}{4\,M_{sun}\,\rho_s^2} \tag{12}$$

4 THEORETICAL TORQUES AND ANGULAR MOMENTA

In this section we will have a look at the theoretical properties of the sun's variable AMm and TRQ corresponding to (5) and its time derivative, respectively. Although we know that the variable AMm could largely lead to energy dissipation instead of building up AMm, we will nevertheless satisfy ourselves by only considering (5) as if the AMm really varies that way. However, the corresponding TRQ acts in a pervading way on the solar body and may influence the rotational behavior more easily when closer to the solar spin axis, because rotational inertia increases quadratically as a function of the distance from that axis. The dependence upon mass density is only linear in this respect. Two plots containing the spin components and one equatorial component of AMm and TRQ, covering each half of the period 1730-2010, are provided as Figs. 1 and 2 (all figures representing plots are attached at the end). Although the presence of the equatorial components of the TRQs is of paramount importance for the medium and long term dynamical behavior of the sun, the analysis of this aspect is not part of the present study.

The conventional orthogonal sun co-ordinates we have employed have their z-axis on the solar spin axis. The assumed sun spin axis in ecliptic coordinates (1950) has a colatitude of 7.15^0 and a right ascension of 284.93^0. The x-axis on the side of the vernal equinox is located in the plane containing the spin axis and the ecliptic z-axis. The y-axis then coincides with the direction towards the ascending node of the solar equator with respect to the ecliptic. The equatorial component of AMm and TRQ shown in Figs. 1 and 2 are limited to the x-axis. The component on the y-axis is still smaller.

4.1 Amplitudes of the Variable Solar AMm

To start with, we want to estimate an upper limit for the magnitude of the mixed moments. Assuming coplanar circular orbits and all Jovian planets aligned we find the approximate maximum components perpendicular to the ecliptic by evaluating :

$$\sup M_{sun}\,|p_{ij}| \;\approx\; M_{sun}\,\frac{2\,\pi m_i\,m_j\;a_i\,a_j}{365}\,(\frac{1}{T_i}+\frac{1}{T_j}) \tag{13}$$

where the values of a_i and the sidereal orbital periods T_i are given in the appendix. The value $2\pi\,a_i/(365\,T_i)$ approximates the mean scalar tangential velocity of planet i. For Jupiter combined with Saturn we find $0.9207\ 10^{-02}$ in plotting units, $0.2303\ 10^{-02}$ when combined with Uranus and with Neptune we get $0.4012\ 10^{-02}$. Saturn together with Uranus yields $0.602\ 10^{-03}$ and with Neptune $0.975\ 10^{-03}$. Finally, for Uranus and Neptune we get not more than $0.135\ 10^{-03}$. The sum of all these values is equal to $1.724\ 10^{-02}$ and has to be compared with $|\mathbf{D_{sc}}| = 1.35\ 10^{-2}$ mentioned in (3). It is thereby obvious that there are special orbital configurations of the Jovian planets which can in principle yield a $\mathbf{B_{var}}$ whose value can reach $-\mathbf{D_{sc}}$. It is further interesting to note that the constant AMm of the Jupiter orbit around the sun is approximately equal to $1.19\ 10^{-1}$ in plotting units. Thus, larger by a factor 7 than the maximum variablesolar AMm. In general, the values of the TRQs are approximately thousand times smaller than the variable AMm.

Table 2. Dates and sizes of AMm Extrema

Ref.	AD AT MIN	ANG MOM AT MIN	ΔT TO MAX	ANG. MOM. AT MAX	ΔT MIN TO MIN	PERIOD LENGTH
θ	1601.92	-0.083 e-01	14.50	0.077 e-01	8.41	22.91
η	1624.83	-0.146 e-01	7.84	0.137 e-01	7.91	15.57
ζ	1640.58	-0.096 e-01	15.67	0.102 e-01	8.17	23.84
ϵ	1664.50	-0.164 e-01	7.42	0.130 e-01	7.83	15.25
δ	1679.75	-0.078 e-01	15.17	0.094 e-01	8.41	23.58
γ	1703.33	-0.140 e-01	8.92	0.105 e-01	11.0	19.92
β	1723.25	-0.064 e-01	10.08	0.092 e-01	8.59	18.67
α	1741.92	-0.102 e-01	10.16	0.079 e-01	11.5	21.66
a	1763.58	-0.103 e-01	9.09	0.121 e-01	7.91	17.00
b	1780.58	-0.095 e-01	15.09	0.075 e-01	8.33	23.42
c	1804.00	-0.147 e-01	7.50	0.140 e-01	8.00	15.50
d	1819.50	-0.112 e-01	18.87	0.092 e-01	4.96	23.83
e	1843.33	-0.157 e-01	7.67	0.127 e-01	7.75	15.42
f	1858.75	-0.083 e-01	14.75	0.085 e-01	8.58	23.33
g	1882.08	-0.128 e-01	9.09	0.104 e-01	10.75	19.84
h	1901.92	-0.070 e-01	10.25	0.099 e-01	8.50	18.75
i	1920.67	-0.102 e-01	9.66	0.072 e-01	12.42	22.08
j	1942.75	-0.103 e-01	8.75	0.127 e-01	7.92	16.67
k	1959.42	-0.109 e-01	15.50	0.071 e-01	8.25	23.75
l	1983.17	-0.145 e-01	7.25	0.140 e-01	7.91	15.16
m	1998.33	-0.122 e-01	15.58	0.083 e-01	8.25	23.83
n	2022.17	-0.146 e-01	8.00	0.125 e-01	7.83	15.83
o	2038.00	-0.086 e-01	14.00	0.079 e-01	8.83	22.83
p	2060.83	-0.117 e-01	9.25	0.102 e-01	10.59	19.84
q	2080.67	-0.073 e-01	10.41	0.100 e-01	8.42	18.83
r	2099.50	-0.105 e-01	9.00	0.077 e-01	13.58	22.58
s	2122.08	-0.105 e-01	8.17	0.133 e-01	8.08	16.25

The AMm values in our plots are systematically multiplied by 10^4 while for TRQ values we employed the factor 10^7. Nevertheless, Figs. 1 and 2 do not allow to appreciate the exact magnitude and date of occurrence of regularities and irregularities hidden in the theoretical periods and amplitudes. Therefore, we have compiled table 2 containing epochs (AD or 'Anno Domini') of the AMm at minimum and the time difference ΔT to the AMM maximum each time with the AMm value at these occurrences. For easy reference we add ΔT corresponding to the duration from maximum to minimum in the last but one column and thereafter the period length (minimum to minimum) valid for a line. The first column contains an identification character for easy reference to a given AMm period. The 'secondary' maxima and minima preceeding an AMm maximum, like for instance between 1820 and 1835 as well as between 1960 and 1975, are not reported in Table 2, although the corresponding effect of the secondary extrema on the TRQs is quite important.

Inspecting the plots, one observes a few large AMm excursions between successive extrema

which are worth to be looked at more closely. In table 2 we identify them as the AMm periods η, ζ, ϵ of the seventeenth century, the periods c,d,e in the nineteenth century and finally at the periods l,m,n corresponding to the present. These periods are selected by searching any two successive extrema which have AMm values which, by adding their absolute values, exceed 0.0250. For the η, ζ, ϵ periods we get:
Min $\rightarrow$ Max at 1624.83 $\rightarrow$ 1632.67 with AMm $-0.14610^{-01} \rightarrow +0.13710^{-01}$ in 7.84 yr
Max $\rightarrow$ Min $\rightarrow$ Max at 1656.25 $\rightarrow$ 1664.42 $\rightarrow$ 1671.92 with AMM $+0.102\ 10^{-01} \rightarrow$
$-0.164\ 10^{-01} \rightarrow +0.130\ 10^{-01}$ in 15.67 yr where $-0.164\ 10^{-01}$ in 1664.42
is the largest isolated single AMm extremum between 1600 and 2130.
In the nineteenth century we find:
Min $\rightarrow$ Max $\rightarrow$ Min at 1804.00 $\rightarrow$ 1811.50 $\rightarrow$ 1819.50
with AMm $-0.147\ 10^{-01} \rightarrow +0.140\ 10^{-01} \rightarrow -0.112\ 10^{-01}$ in 15.50 yr
Min $\rightarrow$ Max at 1843.33 $\rightarrow$ 1851.00 with AMM $-0.157\ 10^{-01} \rightarrow +0.127\ 10^{-01}$ in 7.67 yr
From the periods l,m,n we extract:
Min $\rightarrow$ Max $\rightarrow$ Min at 1983.17 $\rightarrow$ 1990.42 $\rightarrow$ 1998.33
with AMm $-0.145\ 10^{-01} \rightarrow +0.140\ 10^{-01} \rightarrow -0.122\ 10^{-01}$ in 15.66 yr
Min $\rightarrow$ Max at 2022.17 $\rightarrow$ 2030.17 with AMm $-0.14610^{-01} \rightarrow +0.125\ 10^{-01}$ in 8.00 yr
One can verify that the time difference of two successive first extrema of the three periods just described, is equal to 178.5 ± 1 yr. The time between any two of these large extrema is always equal to 7.5 ± 0.5 yr.

4.2 AMm Half and Full Period Variations

Although not included for inspection in table 2, we have counted the zero transitions of the z-components of the ecliptic AMm (Bz) from 1758.58 up to 2002.92. We got 26 occurrences, corresponding to 12.5 full periods which leads to an average of 19.55 yr. The overall mean of the AMm periods in the last column of table 2 is 19.87 yr or equal to (T_{56}) within 0.01 yr. This last number may suggest a regularity in the periods which *is* in fact *not* present at all. The prime purpose of table 2 – actually derived from the Bz behavior – is to make this clearly visible.

Considering the whole time interval covered by table 2, we notice that the succession of the separate Bz periods exhibits an alternation of 15 shorter periods in an interval from 15 to 20 yr on one hand, a hole of 1.5 yr and thereafter 12 periods lasting up to 24 yr on the other hand. But there is more! The separation of a minimum from the next maximum has the larger average, namely 11.27 yr, compared to the mean time interval separating a maximum to the next minimum which only amounts to 8.6 yr. This means that there is a larger pure statistical probability to find two AMm extrema with a leading maximum in one and the same sun spot activity cycle, rather than the reverse. This is what happened in the cycles 6, 8 and 13. The reverse did not occur between 1755 and today.

In contrast, the opposite applies to the probability to find a solar maximum. First, these maxima are *always* present in the longer AMm half period. However, solar maxima are missing in 4 shorter half periods, namely in between Bz maximum in cycle 4 and the minimum in cycle 5, Bz maximum in cycle 9 followed by the minimum in cycle 10, the same between cycle 11 and 12 as well as in cycle 22 and 23, all in the period from 1755 till today. Second, it even occurred in this time interval that two solar maxima occurred in

one and the same half period from minimum to maximum Bz, namely in the cycles 10 and 11 and obviously also now if the expected solar maximum does not occur beyond 2013.92, which is the next Bz maximum. The latter was preceded by the Bz minimum at 1998.33 which was followed by two intermediate secondary Bz extrema where Bz remained positive but larger than the Bz absolute maximum of 2011.50. Also the last but one case (cycle 10 to 11) was accompanied by two secondary extrema with negative values, just like that what happens at present.

We further observe that the absolute values of the variable AMm sizes generally alternate in magnitude from one extrema to the next from higher to lower and the reverse. Thus, altogether a handful observations displaying an obvious similarity with the effect described by Gnevychev and Ohl(1948).

4.3 Location of the Three-foil Episodes Between 1600 and 2130

Scrutinizing Table 2 one observes the almost equality of the full AMm period durations (γ, β), (g,h) and (p,q) of table 2. These periods more or less coincide with the geometrical three-foils obtained by projecting the sun's trajectory onto the ecliptic. In fact, we are not really interested in the geometrical three-foils, but rather in the AMm similarities occurring during a longer time and separated by $\approx$ 178.75 yr. The graphical and the dynamical three-foil intervals largely, but not completely overlap. We nevertheless retain the name three-foil episode to also refer to such complete particular dynamical periods.

Table 3. AMm·10^4 Maxima and Minima During Three-foil Episodes

AD Max 1	AD Min 1	AD Max 2	AD Min 2	AD Max 3	AD Min 3	AD max 4
AMm/ΔT	AMm/ΔT	AMm/ΔT	AMm/ΔT	AMm/ΔT	AMm/ΔT	AMm
1712.25	1723.25	1733.33	1741.92	1752.08	1763.58	1772.67
105/11.00	-64/10.08	92/8.59	-102/10.16	79/11.50	-103/9.09	121
1891.17	1901.92	1912.17	1920.67	1930.33	1942.75	1951.50
104/10.75	-70/10.25	99/8.50	-102/9.66	72/12.42	-103/8.75	127
2070.08	2080.67	2091.08	2099.50	2108.50	2122.08	2130.25
102/10.69	-73/10.41	100/8.42	-105/9.00	77/13.58	-105/8.17	133

we now have to define similarity. Therefore we introduce strict limits on the values of the successive AMm extrema to compare, which shall be equal within 0.001 in plot units. In contrast, differences in successive ΔT values are accepted up to approximately 1. yr. This leads to Table 3.

By inspecting the ΔT values in Table 3, we see that the difference of absolute time increments in the three first columns are always smaller than 0.25 yr from one episode to the next, thus up to and including the 'Max 2' column. Notwithstanding, we have to include the fourth column in what we will call the 'strict Similarity Episode', because it is involved in the ΔT of column three and moreover, the difference between the epochs inside the fourth column are still within 0.08 yr from the approximate **S**mallest **C**ommon **M**ultiple **P**eriod (SCMP) of 178.5 yr. What follows beyond the second minimum shows a clear divergence in time similarity but the successive AMm amplitudes still remain closely

comparable. The period starting from the second minimum can therefore be called 'Diverging Similarity Episode'. The duration of both episodes combined, or the dynamical three-foil episode amounts to 60.3 ± 0.13 yr in total.

The three geometrical three-foils corresponding to table 3, all approximately start at the AMm zero in between the first minimum and second maximum of table 3. These three-foils end at the AMm zero following the AMM maximum four, relying on the data from Charvatova's(2000) paper. The duration of the geometrical three-foil episodes is approximately 50 yr. The duration difference between the geometrical and dynamical three-foil episodes is just due to the addition of the full initial AMm period in the latter case.

5. TRQs AND ENERGY VERSUS SUN SPOT ACTIVITY

In this section we will compare essentially the graphical properties of theoretical data with sun spot activity in combined plots. To this end Figs. 1 and 2 already contain at their bottom the conventionally smoothed sun spot activity data. To this we add the plots in the Figs. 3, 4 and 5 which are dedicated to theoretical energy values compared to detailed softly smoothed monthly activity counts sampled four times a year. If ACT(i) is a monthly mean sunspot record for month i, the softly smoothed count SACT(i) is defined by SACT(i)=0.25(ACT(i-1)+2ACT(i)+ACT(i+1)). The purpose is to safeguard the fine structure of activity peaking occurrences in a context of four samples per year.

In a number of instances we will provide mean values. Taking into account that the samples we deal with, are very small, we will represent most of the mean values by the bracket $[a < b < c]_n$, where a is the lowest value found in the sample, b is the arithmetic mean and c is the largest value for a sample of n recorded values. Standard deviations, if computed, are denoted by σ.

5.1 Solar Activity Maxima and TRQ Extrema

A punctual identification of a solar maximum is not feasible, because a solar maximum is not a precise epoch, but a period of variable length and sunspot intensity. The sun spot activity represented at the bottom of the Figs 1 and 2 is based on two samples per year of conventionally smoothed monthly sun spot records. The smoothing process involves 12 months and has a strong low pass filtering effect. Therefore, an activity evolution in a solar cycle having a pronounced maximum will easily be identified. But there are numerous cases where there is no such conspicuous maximum. Nevertheless, a look at the Figs. 1 and 2 confirms the impression that the (intuitive) solar maximum is generally accompanied by an extremum of the spin and x-TRQ components (red curves). Differences up to a few years are very well visible in the cycles 3,8,19 and 22.

Due to the quasi periodicity of AMm and its derivative corresponding to the TRQ, it happens in the majority of instances that the epoch of a TRQ extremum is very close to an AMm zero. Hence, one could alternatively suggest that higher activities are occurring by preference close to AMm zeroes. This is, of course, partly true. After closer verification, it should rather be considered to be a consequence of the quasi periodicity. The cycles 4,7,10,16 and 20 may confirm this.

When looking at the cycles 5,8 and 22 one could ask which of the adjacent TRQ extrema

are now actually closest to the activity maxima. In order to give a simple reply we did cast a glance at sunspot activity peaks. To this aim we also scrutinized the monthly mean sun spot numbers and have not only taken the highest peak of each of the 24 cycles (including cycle zero), but have complemented them with 25 further conspicuous and sufficiently isolated peaks which happen to be distributed in 15 of these 24 cycles. In each cycle separately and for each of the 49 peaks we determined the time difference between the given peak and the closest TRQ extremum inside the cycle. Expressed in years we finally got $[-3.96, 0.53, 4.21]_{49}$ with $\sigma = 2.04$ yr for these time differences. These figures are close to the mean value obtained by only considering in each cycle just the smallest difference. For this smaller sample we obtained $[-3.28, 0.276, 4.21]_{24}$ with $\sigma = 1.96$ yr. We observe that the first peak is best (smallest time difference) in the nine cycles (5),6,7,9,(14),(20),21, and 22. The brackets are added to the cycle numbers, there where a one count difference in the two largest sun spot figures has been disregarded. The highest peak yields the smallest difference in the nine cycles 2,(5),9,10,11,(14),17,(20) and 21. Thus, the cycles (5),9,(14),20 and 21 are represented in both leagues and the union of both sets yields the 11 cycle numbers (5),6,7,9,10,11,(14), 17,(20),21 and 22 or 46% of all cycles analyzed.

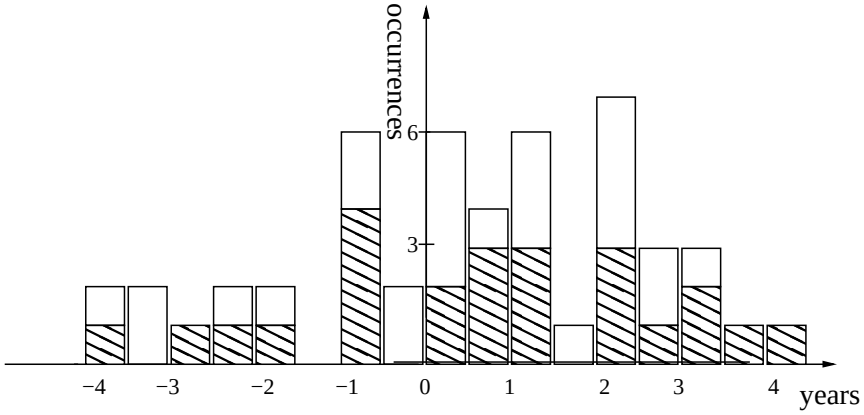

Figure 6. Occurrence density of the 49 separation times between a sunspot number peak and the closest torque extremum. Shaded box parts apply to the highest peak of a given cycle.

A more interesting picture is provided by Fig. 6 showing the occurrence density in boxes representing half a year each. The positive abscissae belong to peaks occurring before the TRQ extremum. The global mean value already mentioned before, is visibly located at approximately 0.5 yr. Quite remarkable are the, not necessarily fortuitous, conspicuous holes at the intervals $(-1.5, -1.0)$ and $(1.5, 2.0)$ yr. A full blown correlation analysis, which may be useful in this case, is outside the scope of the present study.

Also the TRQ zeroes are interesting occurrences, because they could be the start point where a sign reversal of the polar magnetic fields of the sun can develop and contribute to the run down of a cycle. Also that is a subject which might require further attention.

5.2 Energy Periodicities and Cycle Periods

Let us first observe that in the Figs. 3 to 4 the total mass point energy Etot has always its maxima and minima more or less corresponding to a maximum of the approximate body

rotational energy E_{bod} (in red). This is due to the influence of the dot product $\mathbf{B_{sc}} \cdot \mathbf{B_{sv}}$ in (8) on E_{tot} , where $\mathbf{B_{sv}}$ is regularly negative. This dot product can thus cooperate in building the value of E_{tot} or counteract it. The effect will be largest when $\mathbf{B_{sv}}$ has an extremum, but such an extremum turns always into a maximum of E_{bod}. The trace of this counter activity is very well visible as a spike interrupting the minimum of E_{tot} in the cycles 2,9,18 and 22 as well as in between 5 and 6. This peak becomes a hump or only a little bump the higher the E_{tot} minimum occurs. We will come back to the sharp peaks in the next subsection.

If we now look at phase differences between the E_{bod} curve and the activity cycles, we see an almost perfect phase fit in the cycles 3,4,5,19,20 and 22. The E_{bod} curve leans onto the start side or trailing end inside the cycles 1,2,9,10,11,12,15,16,18 and 21. In the 8 cycles left, the phase of the E_{bod} curve drifts partly out of the activity curve and is almost out between the cycles 8 and 9, 13 and 14 as well as between 14 and 15. It is completely out in 1810 (inside the Dalton minimum).

In principle the same comparison applies when employing E_{tot} instead of E_{bod}. We count approximately 13 E_{tot} periods from 1760 until 2000, yielding a mean of 18.4 years. From 1750 to 1810 the odd cycles coarsely correspond to E_{tot} maxima. The opposite is true from 1850 subject to a further change past cycle 14 (1910).

5.3 Deep E_{tot} Energy Minima

By inspecting the energy plot for the nineteenth century (Fig. 3) we were surprised to see that in the middle of the Dalton minimum (±1810) we also had a very low E_{tot} minimum together with the characteristic positive spike already addressed in the previous subsection. Fig. 3 does not really allow to see whether sun spot activity could exhibit a minute trace of an impact due to the E_{tot} behavior. Unexpectedly, a cross check in Fig. 7, where

Table 4. E_{tot} **Minima Between 1600 and 2200**

Start AD End AD	$E_{tot}(min1) * 10^7$ AD	$E_{tot}(max) * 10^7$ AD	$E_{tot}(min2) * 10^7$ AD
1631.29	0.4077	14.75	0.3902
1634.04	1632.21	1632.71	1633.04
1670.88	8.739	17.37	8.001
1674.13	1671.13	1672.04	1672.54
1809.96	0.1000	23.17	0.1124
1813.04	1810.79	1811.29	1812.04
1988.79	0.063	22.37	0.047
1992.04	1989.63	1990.46	1990.96
2129.04	2.903	11.84	2.909
2131.38	2129.79	2130.29	2130.54
2167.71	0.023	16.84	0.004
2170.96	2168.71	2169.38	2169.79

the monthly mean spot counts are divided by three, shows that there is such an impact pointing to a relatively direct relation. The plot in Fig. 7 suggests two questions. Is the

descent to the E_{tot} minimum at the origin of a decay of sun spot occurrences? is one question. Does the spike contribute to the restoration of sun spot activity, as implied by the incidental cycle activity further in time? is the next question, which can be asked without any speculative consideration in mind.

Motivated by the identification of the 1810 energy minimum we scanned the monthly values of E_{tot} from 1600 until 2200. To this aim we identified the periods where $E_{tot} < 10^{-6}$ in plotting units. The results are shown in Table 4. In this table we give the start and end times of these intervals within the prescribed magnitude bracket. We further provide the epochs and energy values of the two separate E_{tot} minima, as well as the value and epoch of the theoretical spike top in between. We agree to refer to the year of the first E_{tot} minimum to identify the low energy periods in question.

The occurrence of the 1989 E_{tot} minimum occurs right in the middle of the solar maximum period of cycle 22. The activity level of this cycle does not compare at all with the very low activity cycles 5 and 6 around the 1810 minimum. To verify whether the questions asked before have to be abandoned, we produced the plot in Fig. 8. To clean the higher frequency cockscomb from the low frequency signal in the sun spot count curve, we simply subtracted the conventionally smoothed count values from the monthly mean counts. The result oscillates between -40 up to +60 counts but provides a dramatic peak some two to three months beyond the spike maximum. Moreover, this peak corresponds to the highest monthly mean count in cycle 22. Also the surrounding activity count picture shows six peaks whose tops are in a near hyperbolic arrangement around the central spike. They correspond to the 'unsmoothed' peaks occurring at 1988.92, 1989.48, 1990.04, 1991.16, 1991.66 and 1992.16 with the not modified mean monthly counts 179.2, 196.2, 177.3, 167.5, 176.3 and 161.1, respectively. The monthly mean central peak is 200.3 counts high and is one year beyond the conventionally smoothed or low pass filtered activity maximum in July 1989. By the way, R.W. Fairbridge and J.H. Shirley(1987) anticipated a 1989 energy anomaly on the basis of a graphical analysis of the solar trajectory, but the fear they expressed concerning a prolonged minimum, did fortunately not substantiate.

The deep minima of 1810 and 1989 show in both cases a decrease of spot counts in the period preceeding the central spike. This very flat descent extends over more than four years and ends in zero activity in the former case. In the latter case this decrease lasts 1.5 years ending in a deep trough 100 counts below the central activity peak. Beyond the spike something like an activity restoration is initiated in both cases. One thing is clear. The possible energy withdrawal before the spike is modest. It is nevertheless so conspicuous in the 1810 minimum, because it is inside a period of very low activity. A potential energy contribution to sun spot activity coincident with the spike could be substantial, considering the central activity peak of the 1989 minimum. But alternatively, the energy of the spike could merely have triggered the peaking process which is more in line with the 1810 scenario. This is one of the many questions which we have to leave open.

The deep minima in the seventeenth century both occur well inside the Maunder Minimum, see J.C.Ribes and E. Nesme-Ribes(1993) and references therein. Considering the 1989 E_{tot} deep minimum we are led to believe that the E_{tot} minima of 1632 and 1671 are neither at the origin nor a cause of the prolongated sun spot activity black out in the

seventeenth century. Therefore, the two energy lows which will occur in the twenty second century – which, by the way, are mirror images of those of the 17th century – do not necessarily represent an early climatological warning. It may still be interesting to observe that deep minima are closely linked to the SCMP. Referring to table 4 the time differences between spike occurrences of either case 6 minus case 4, or case 4 minus 3 and finally 3 minus 1. All are within ±0.5 yr from 178.75.

5.4 Sun Spot Cycle Patterns

Starting from AMm, TRQs and E_{bod} as well as three-foil episodes, allows us to look for sun spot cycle curve intervals which follow particular patterns which may be linked to conventional dynamics.

The most conspicuous direct pattern similarity we noticed, occurs between the sequence of the sun spot activity in the cycles 1,2,3,4 on one hand and 17,18,19,20 on the other hand, when compared with the simultaneous E_{bod} curve in the Figs 3 and 6. We thereby accept that activity during the early cycles is altogether substantially lower than in the twentieth century. Nevertheless, the highest monthly mean sun spot count in cycle 3 also reached 239 counts (isolated, April 1778), competing with 254 counts in cycle 19 (accompanied by high activity records during many months around September 1957). In the Figs 1 and 2 we observe a very small kink in the descent of negative TRQs around 1750 and a similar slightly more pronounced kink in 1935 and further a very obvious oscillation starting in 1790 as well as in 1967, respectively. It cannot be decided whether the first little bump is the actual start of the sequence, because we have no data before 1745. The 'little oscillations' just mentioned contain in their inside a quick succession of two modest TRQ maxima enclosing a shallow minimum. Looking at the totally different cycles surrounding the deep minima of 1810 and 1989, we may state that the small TRQ oscillation is really occurring at the end of the similarity observed.

Also the cycle sequences 6,7,8 as well as 10,11 have inside such a similar small TRQ oscillation. However, the relative location of the cycle maxima, taken between the large TRQ minima of the oscillation, is so different that no particular similarity is really conspicuous, in contrast with the sequences 3,4 and 19,20.

It remains to be clarified whether the three-foil episodes play some visible role in dynamical parameters and solar activity. With this question in mind, we had defined a 'strict similarity episode' at the end of section 6.4. According to table 3 this period coincides with the cycles 13,14,15 and 16, without being able to compare them with life data at a distance of a SCMP into the past. However, this also means that both the sequences 1,2 and 17,18 coincide with the 'diverging similarity episode', also defined in section 6.4.

The simplest way to check direct similarity consists in superposing the curves of sun spot counts of the cycles 17 and 18 with the corresponding curve of the cycles 1 and 2. Taking into account that solar activity levels were much lower in the eighteenth century than in the twentieth, which essentially implies a difference at low frequency level, we subtracted the low frequency conventionally smoothed counts from the monthly mean data points. The first attempt, including cycle 1, had to be abandoned, due to the poor quality of the sun spot counts of cycle 1. Left with the cycles 2 and 18 we selected the epoch of the

third AMm maximum of the two three-foils concerned as common time reference. This is 1763.58 and 1942.75 (see table 3) for cycle 2 and 18, respectively. Although 1763.58 is three years before the end of cycle 1, we are bound to a hypothetical link to both minima of the AMa. Consequently, we must add the same number of years to both start points. We selected two years and Fig. 9 shows 10 years of the superposed plots with the solid curve belonging to cycle 2. Both curves are more or less each other opposite from year 2.1 to short before year 4.5 in Fig. 9, which is a remarkable fact. Thereafter, phase shifts between the activity curves point to small frequency differences and amplitude similarity becomes less conspicuous. Nevertheless, we notice that the large oscillations in the center of the activity zone show a disturbing difference. In cycle 18 there is a clear harmonic magnitude 'decay' starting at year 3.5 and ending just at year 6. In contrast, cycle 2 rather shows a more or less disorderly 'increase' in the same period.

The similarity discovered together with the problem just mentioned, must, in fact, not necessarily be linked to the direct vicinity of the three foil. We therefore plotted the superposition of the next 20 years of higher frequency sun spot counts for the cycles 3 and 4 superposed onto 19 and 20 as well and shown in the Figs. 10 and 11, keeping the same time references mentioned before. Again we see very similar frequencies in both curves with partly opposite magnitudes, very much like at the end of the plots in Fig. 9. But the decay in amplitude of the high frequency activity curves of cycle 2, 3 and 4 look very similar to those of the 18, 19 and 20, respectively. The speculative thought saying that 'at its end a three-foil brings the sun in a activity state comparable to the state at the previous three-foil end' seems confirmed by the present observations. This clearly suggests an impact from dynamics onto short term solar activity, where short term means a few decades.

CONCLUSIONS

The major part of this note concerns the screening of the analytical description of the variable angular momentum of the sun as mass point. The link made between this angular momentum and the solar body is important to allow the assumption that the sun undergoes corresponding true body torques. The proposed relation is still a conjecture claiming that 'the variable angular momentum of a mass point representing a body of the solar system requires a body angular momentum of equal size and opposite sign to guarantee the constancy of the angular momentum of the full solar system'. The conclusions presented hereafter thus concentrate on variable angular momenta, torques and solar activity which, do not always require the application of the proposed 'mass point - body link'. Especially energy considerations are unaffected by the conjecture just mentioned.

On the other hand, periodicity considerations valid for torques acting on the sun rely on the proposed mass point - body link. The first consequence is that the basic frequency of the different torques acting onto the sun are only due to the planets acting in pairs with their specific synodic periods. A complementary observation is the fact that the time span separating simultaneous conjunction of the pair Jupiter/Saturn and the conjunction of Uranus/Neptune is 22.46 yr, the Hale cycle period. Exactly the same period applies to the pairs Jupiter/Uranus and Saturn/Neptune.

The three-foils, known from the graphical analysis of the solar trajectory and known to be subject to the 178.50 yr periodicity, coincide with periods of similar theoretical angular momentum and torque parameters. A verification based on the superposition of higher frequency sun spot activity curves of the cycles 3, 4 and 5 onto the cycles 18, 19 and 20, respectively, indicate that the sun spot activity immediately beyond the three-foils is subject to a slowly decaying similarity.

It is further noteworthy that a very basic and un-differentiated approximation of the sun body rotational energy only based on the variable angular momentum, provides a curve with a slightly variable periodicity being more or less in phase with more than 60% of the 24 recorded sunspot cycles.

The total mass point kinetic energy shows two deep theoretical minima occurring in 1810 and 1989. Although valid for the mass point, these minima nevertheless seem to give rise to an influence on sun spot behavior around the center of these minima. This influence may point to pseudo tides in the solar interior accompanying the accelerations which are a byproduct of the variable mass point angular momentum.

As far as the analysis goes, no immediate link was observed between the sun spot activity amplitude and the proposed variable rotational dynamics applicable to the solar body.

ACKNOWLEDGMENT

I am very much indebted to Fréderic Clette for guiding me through the relevant literature of solar physics.

APPENDIX

The parameters shown hereafter are extracted from the pocket atlas by J. Hermann(2000).

Orbital Parameters of the Major Planets

	a(AU)	e	M(EM)	Sidereal Period(yr)	Inclination (deg)
Mercury	0.387	0.206	0.055	0.241	$7^0\,0.3'$
Venus	0.723	0.007	0.815	0.615	$3^0\,23.7'$
Earth	1.000	0.017	1.000	1.000	–
Mars	1.524	0.093	0.107	1.881	$1^0\,51.0'$
Jupiter	5.203	0.048	317.89	11.862	$1^0\,18.3'$
Saturn	9.539	0.055	95.18	29.458	$2^0\,29.3'$
Uranus	19.191	0.047	14.54	84.015	$0^0\,46.3'$
Neptune	30.061	0.010	17.13	164.79	$1^0\,46.3'$

REFERENCES

Abreu J.A., Beer J., Ferriz-Mas A., McCracken K.G. and Steinhilber F., 2012,'Is there a Planetary Influence on Solar Activity', Astronomy & Astrophysics, 548, A88, DOI: 10,1051/0004-6361/201219997

Anderson C.N.,1954,'notes on the Sunspot Cycle',J. of Geophysical Research, 59,4, 455

Charbonneau P.,2010, 'Dynamo Models of the Solar Cycle', Living Rev. Solar Phys. 7(2010),3
Charvatova I. and Stŕeštík J.,1991, 'Solar Variability as a Manifestation of the Sun's Motion', J. Atmospheric and Terr. Phys., 33(11-12), 1019
Charvatova I.,2000. Can the Origin of the 2400-year Cycle of Solar Activity be Caused by Solar Inertial Motion. Ann. Geophys. 18, 399
de Jager C. and Versteegh G.J.M.,2005. Do Planetary Motions Drive Solar Activity. Solar Phys., 229, 175
Fairbridge R.W. and Shirley J.H.,1987. Prolonged Minima and the 179-yr Cycle of the of the Solar Inertial Motion. Solar Phys., 110, 191
Beck J.G. and Giles P.,2005. Helioseismic Determination of the Solar Rotation Axis. The Astrophys. J., 621, L153.
Gnevyshev M.N. and Ohl A.I.,1948. On the 22 Year Cycle of Solar Activity. Astron. Zh., 25, 18
Herrmann J.,2000. dtv-Atlas Astronomie. Deutscher Taschenbuch Verlag, fourteenth modified and corrected Ed., München,
Howe R.,2009. Solar Interior Rotation and its Variation. Living Rev., Solar Physics, 6(2009),1
Jose P.D.,1965. Sun's Motion and Sun Spots. Astron. J., 70, 193
Jucket G. A.,2003. Temporal Variations of Low-Order Spherical Harmonic Representations of Sunspot Group Patterns: Evidence of solar spin-orbit Coupling. Astronomy and Astrophys., 399, 731
Lang K.R.,2000, The Sun from Space. Springer, Heidelberg
Ribes J.C. and Nesme-Ribes E.,1993, The Solar Sunspot Cycle in the Maunder minimum AD 1645 to AD 1715. Astron. Astrophys., 276, 549
Wilson I.R.G., Carter B.D. and White I.A.,2008. Does a Spin Orbit Coupling Between the Sun and the Jovian Planets Govern the Solar Cycle?. Publ. Astr. Soc. of Australia, 25, 85.
Wilson P.R., 1994, Solar and Stellar Activity Cycles, Cambridge University press, Cambridge(UK).

FIGURES

Figures with curve plotting are attached in the next pages.

FIGURE 1, Spin, equatorial X AMM and TRQ of
the Sun in the Period 1730 till 1870 with
smoothed solar activity on the bottom line

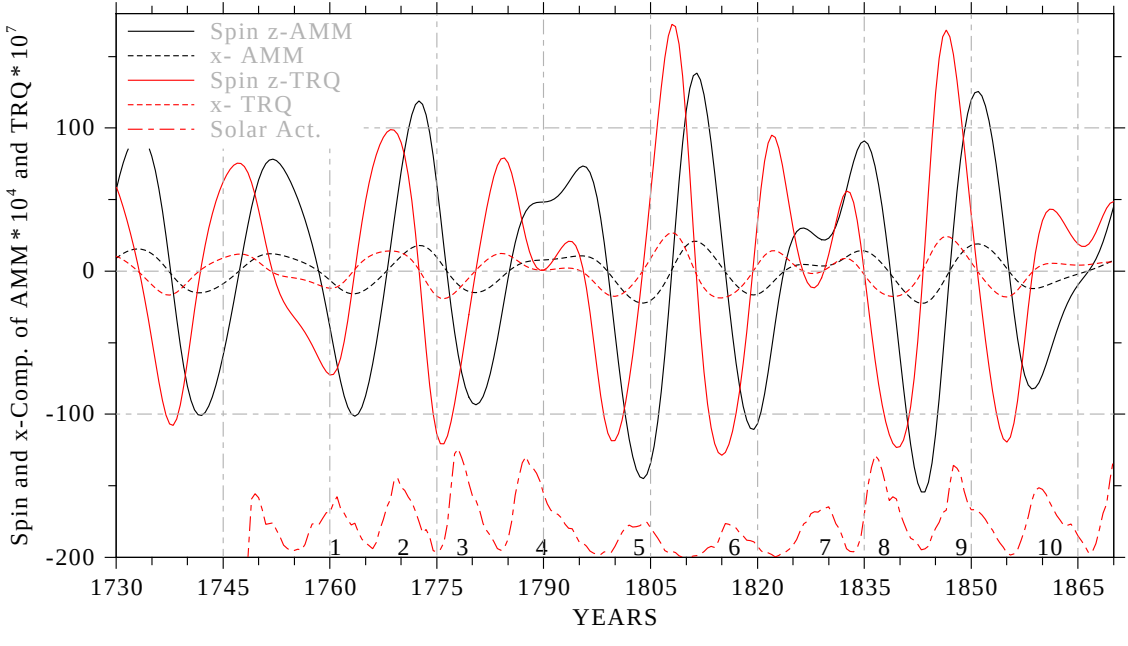

Fig.2. Spin and equatorial X AMM and TRQ
of the Sun in the Period 1870 till 2010
with smoothed sol. act. on the bottom line

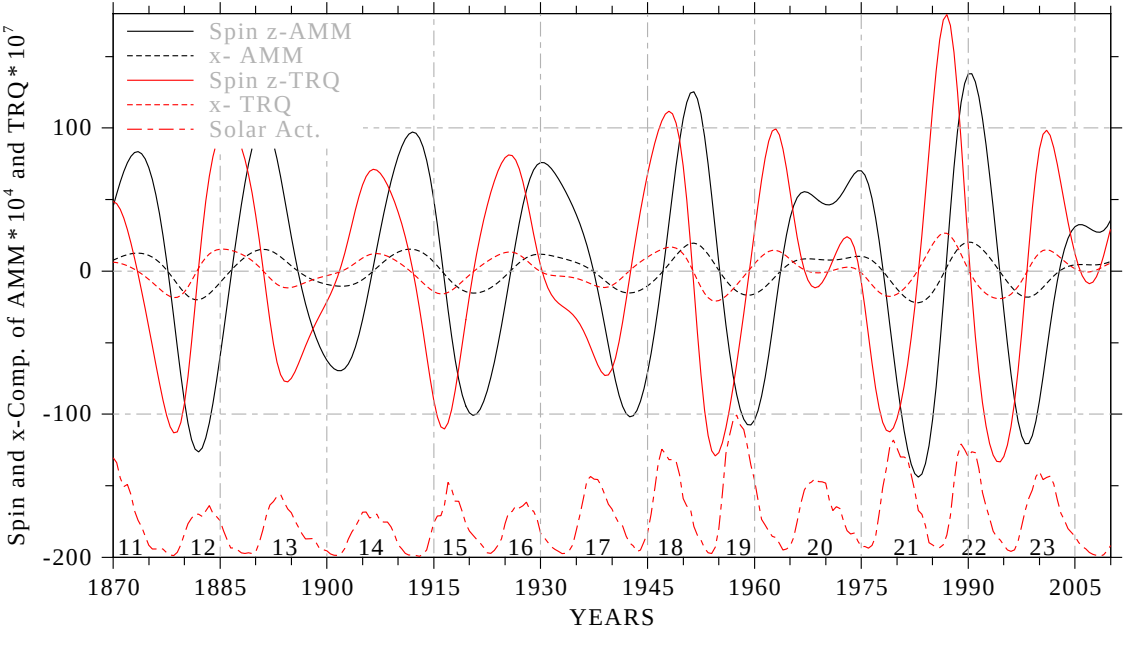

Fig. 3. Activity Count and Rotational
Energy Types E(total) and E(body)
from 1750 to 1840

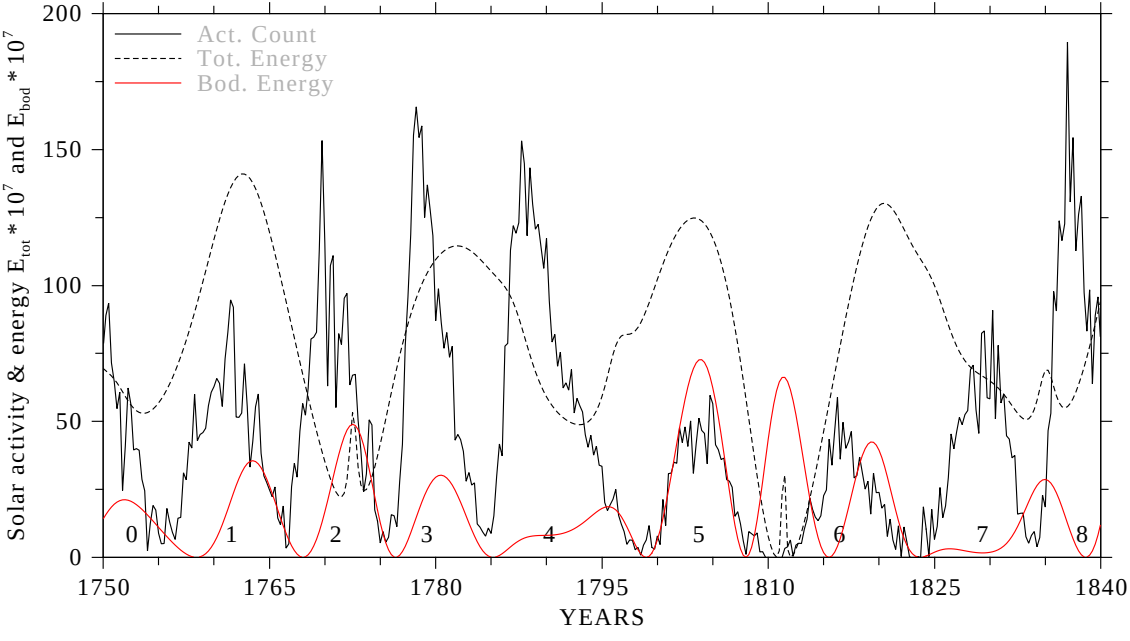

Fig. 4. Activity Count and Rotational
Energy Types E(total) and E(body)
from 1840 to 1930

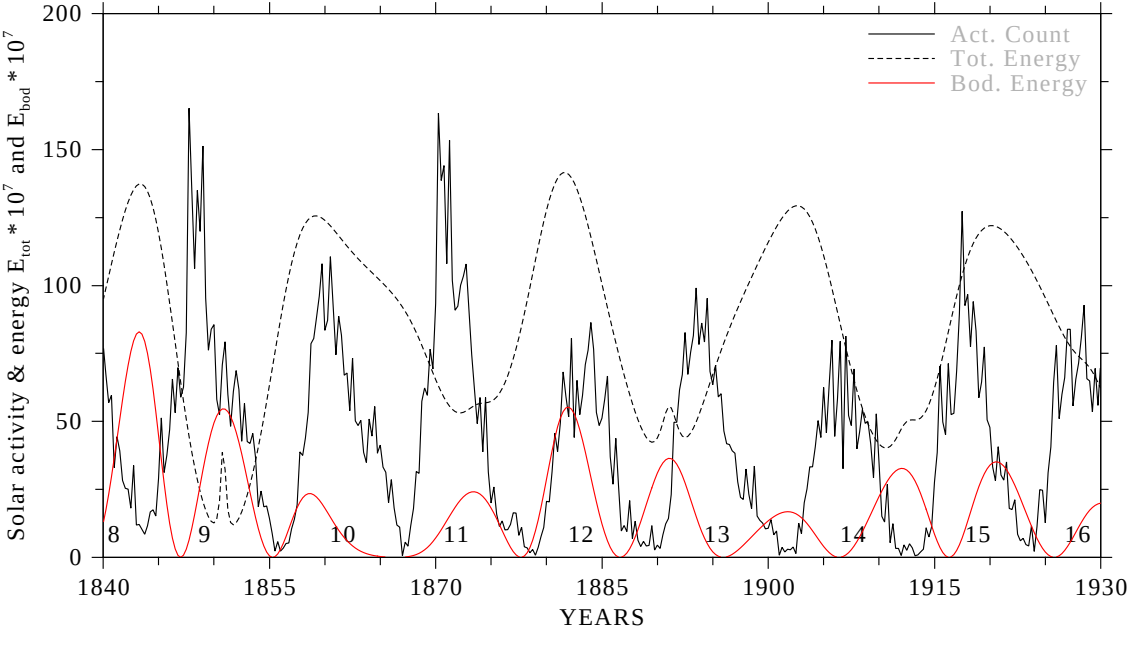

Fig. 5. Activity Count and Rotational
Energy Types E(total) and E(body)
from 1920 to 2010
(Fig. 6 incorporated inside the text)

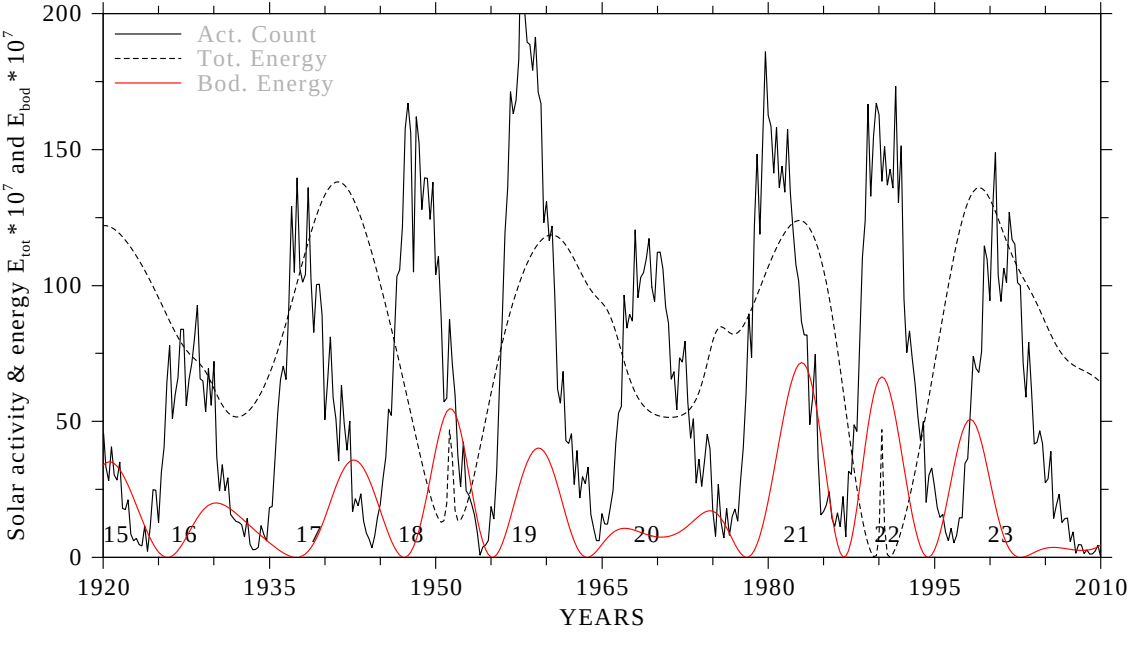

Fig. 7. Unsmoothed Sun Spot Counts compared with
Rotational Energy Etot at the Deep 1811 Minimum

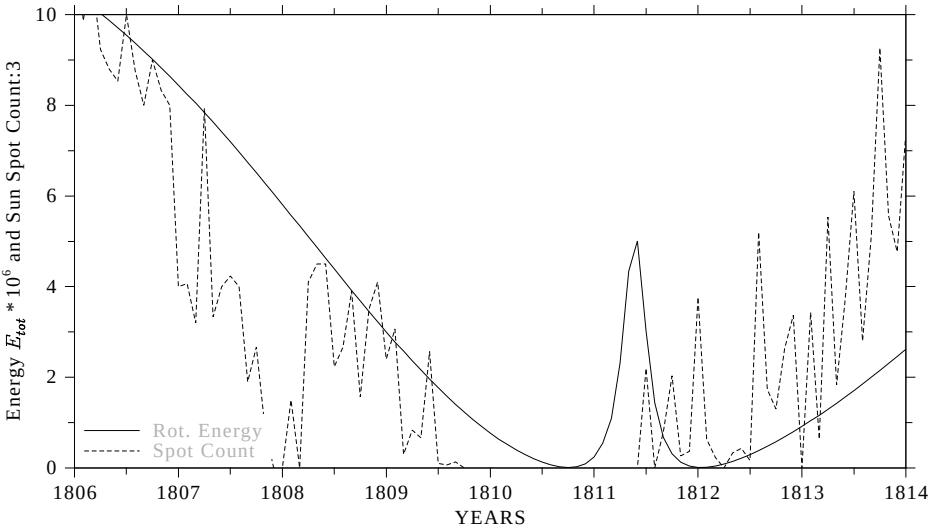

Fig. 8. Comparison of unsmoothed MINUS smoothed
Sun Spot Counts (-40 to +60), with rotational
energy at the deep energy minimum of 1990

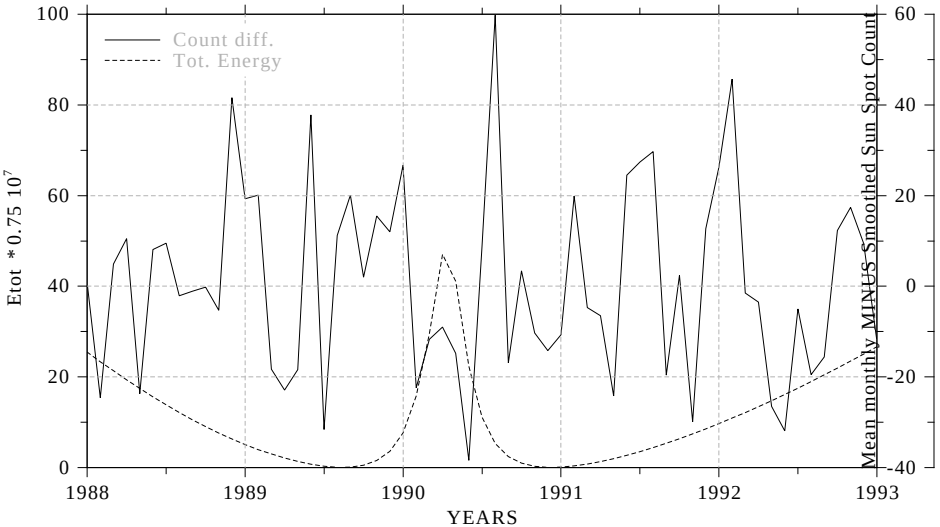

NOTE 9C

Fig. 9. Superposition of Cycle 2 and 18

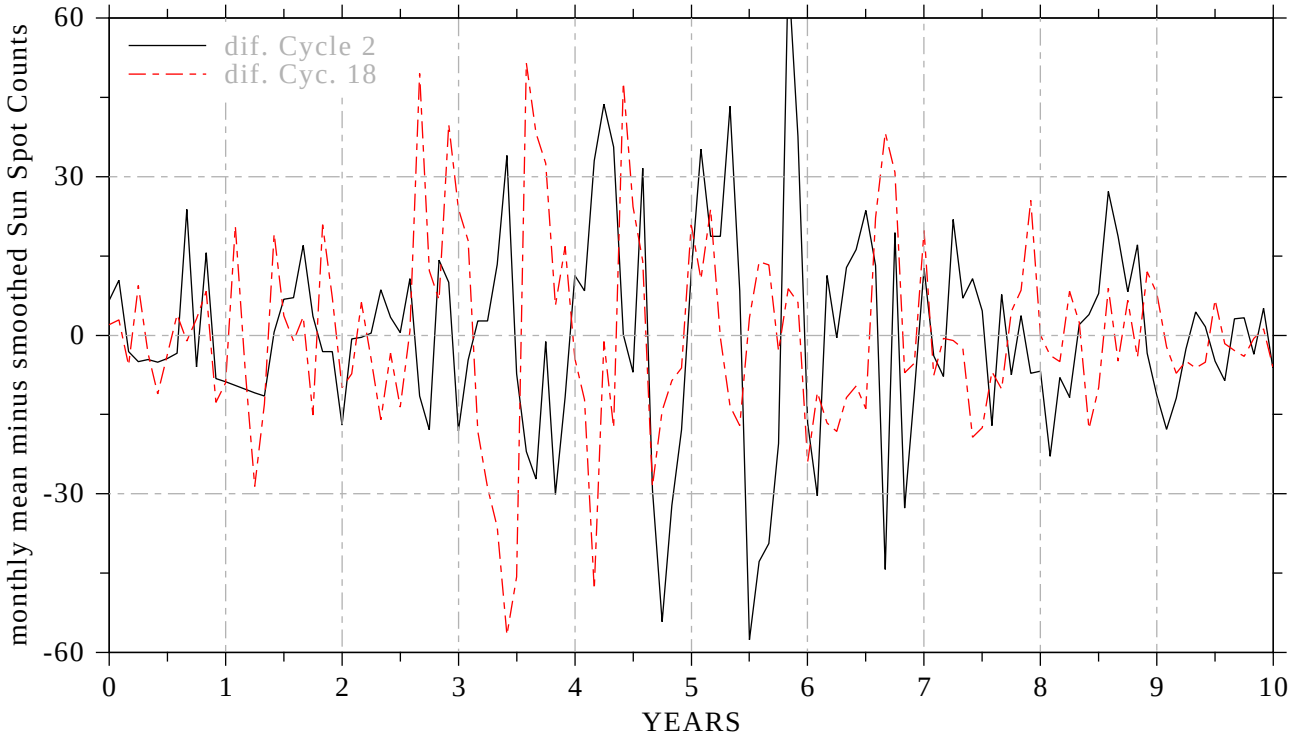

NOTE 9C

Fig. 10. Superposition of Cycle 3 and 19

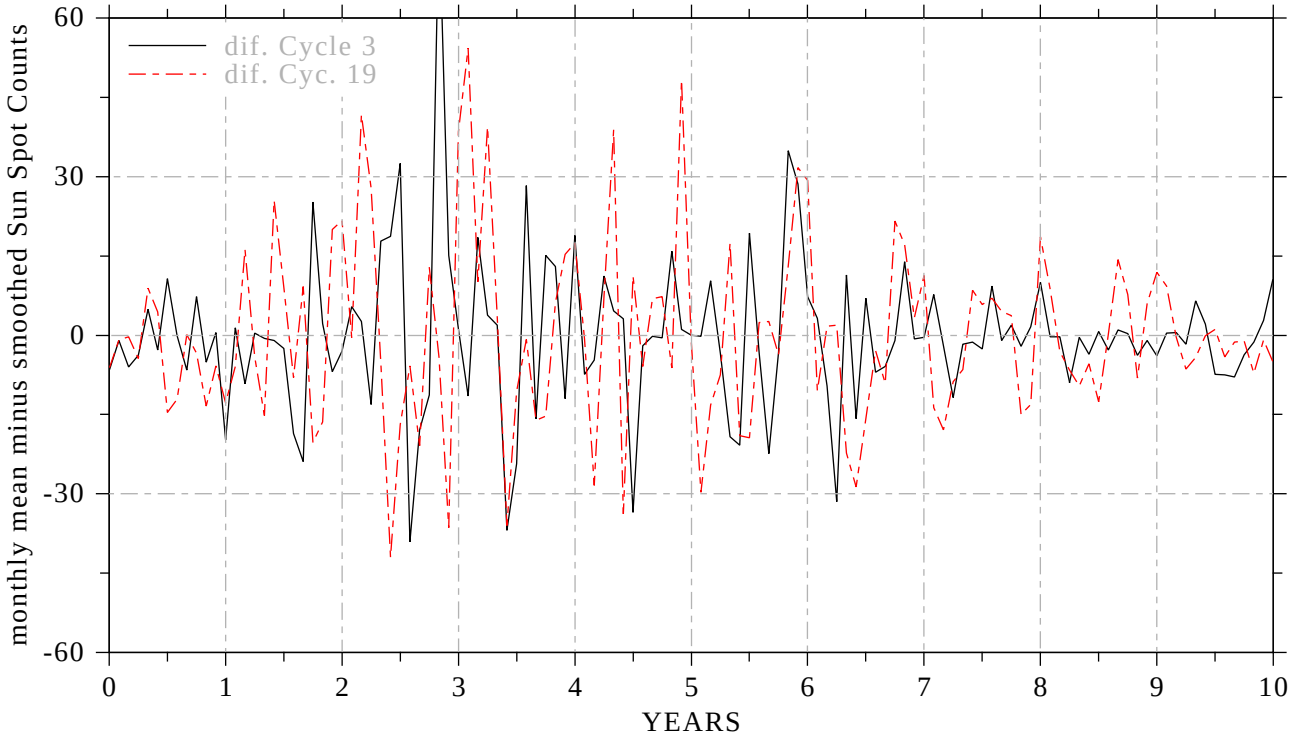

NOTE 9C

Fig. 11. Superposition of Cycle 4 and 20